

MILLIMETER RADIO ASTRONOMY AND THE SOLAR CONVECTION ZONE

O. V. Arkhypov^{*†}, O. V. Antonov^{*†}, and M.L. Khodachenko[‡]

Abstract

The global distribution of solar surface activity (active regions) is connected with processes in the convection zone. To extract the information on large-scale motions in the convection zone, we study the solar synoptic charts (Mount Wilson 1998-2004, Fe I, 525.02 nm). The clear indication of large-scale ($\geq 18^\circ$) turbulence is found. This may be a manifestations of the deep convection because there is no such global turbulent eddies in the solar photosphere. The preferred scales of longitudinal variations in surface solar activity are revealed. These correspond to $\sim 15^\circ$ to 51° (gigantic convection cells), 90° , 180° and 360° . Similar scales (e.g., 40° and 90°) are found in the millimeter radio-images (Metsähovi Radio Observatory 1994-1998, 37 and 87 GHz). Hence, the millimeter radio astronomy could prove useful for remote sensing of the solar convection zone.

1 Introduction

Numerous attempts to detect photospheric manifestations of deep convection (mainly gigantic cells) were carried so far with no definitive results [Williams and Cuntz, 2009]. That is why the consideration of new approaches in that respect seems to be an actual task. Microwaves give valuable information on activity in the solar chromosphere. Although the Nobeyama synoptic maps of solar radio emission at 1.8 cm wavelength (17 GHz) are available online, firstly we consider the millimeter emission (3.4 mm and 8 mm; Metsähovi Observatory) from more deep levels of the chromosphere. There are promising results of the previous studies with this approach [Brajša et al., 1992; Vršnak et al, 1992]. The goal of this work is the new argumentation for using of mm-data in investigations of the convection zone.

^{*} *Institute of Radio Astronomy, Ukrainian Academy of Sciences, Chervonopraporna 4, 61002, Kharkiv, Ukraine*

[†] *Department of Space Radio Physics, Kharkiv V. N. Karazin National University, Svoboda Square 4, 61077 Kharkiv, Ukraine*

[‡] *Space Research Institute, Austrian Academy of Sciences, Schmiedlstrasse 6, A-8042 Graz, Austria*

Active regions on the solar surface are generally thought to originate from a strong toroidal magnetic field generated by a deep seated solar dynamo mechanism operating at the base of the solar convection zone [Tobias, 2002]. The magnetic fields need to traverse the entire convection zone before they reach the photosphere to form the observable solar active regions. The numerical modeling predicts the turbulence in the convection zone forming loop structures of magnetic flux tubes which emerge as active regions above giant cells [Laurène and Brun, 2009]. Hence, the convective deformation of large-scale magnetic structures above the tachocline could be imprinted in the surface magnetic field and global distribution of active regions.

By this, surface signatures of the transport of the magnetic field could be used as a probe of the solar convection zone. We are looking for the manifestations of deep, large-scale turbulent convection in optical data and mm-data.

2 Turbulence in Large-scale Pattern of Active Regions

The Kolmogorov's theory of turbulence (e.g., Lang [1974]) predicts the universal relation between the characteristic length-scale of turbulent eddies (L) and the time scale of their variability (τ_L): $\tau_L \propto L^{2/3}$.

To examine this relation in the solar activity pattern, we study the synoptic charts of the intensity of the Fe I spectral line (5250.2 Å), which are constructed from the digital data obtained at the 150-foot Tower Telescope at Mount Wilson in 1998-2004 (ftp://howard.astro.ucla.edu/pub/obs/synoptic_charts/PDF_files/).

We use these charts in equidistant cylindrical projection (Figure 1a) for the period of high activity (1937-2021 Carrington rotations, i.e. between 7 June 1998 and 12 October 2004). For each line at a given latitude ϕ in the chart we calculate the individual Fourier spectrum with the step of $\phi = 0.5$ deg. Such spectra of longitude variations of solar activity were averaged over all latitudes in the chart (Figure 1b). Averaged spectra differ from one chart to another. To estimate the time-scale of the variation, we calculate the autocorrelation of the spectral parameter (the squared amplitude, divided by the average squared amplitude of the harmonics with $1 \leq m < 30$, or the phase of a harmonic). The peak of the autocorrelation coefficient r_t at short time lags t can be approximated by the relation: $r_t = \exp(-t/\tau)$. Hence, the time-scale of harmonic variability can be estimated as: $\tau = P/\ln(r_{t=P})$, where $P = 27.28$ days is the average time interval between mapping of one detail in successive charts or one synodic period of the solar rotation.

Figure 2a shows the time scale τ for harmonics with different periods in longitude defined as $\frac{360^\circ}{m}$, where $1 \leq m \leq 20$ is the harmonic number. The squared amplitudes of the harmonics were used for estimation of τ with the above described autocorrelation method. It is remarkable that the $\tau(m)$ can be approximated with the regression: $\lg \tau = C + \alpha \lg m$, where $C = 0.47 \pm 0.07$ and $\alpha = -0.65 \pm 0.08$. Applying the same approach to the phase of harmonics reveals a similar result of $\alpha = -0.65 \pm 0.12$ for the northern hemisphere and $\alpha = -0.69 \pm 0.11$ for the south. Taking the average value for α , one can finally write: $\tau \propto m^\alpha = m^{-0.66 \pm 0.06}$, which is, in view of $L = 360^\circ/m$, consistent with the turbulence theory, giving $L^{2/3} \propto m^{-0.67}$.

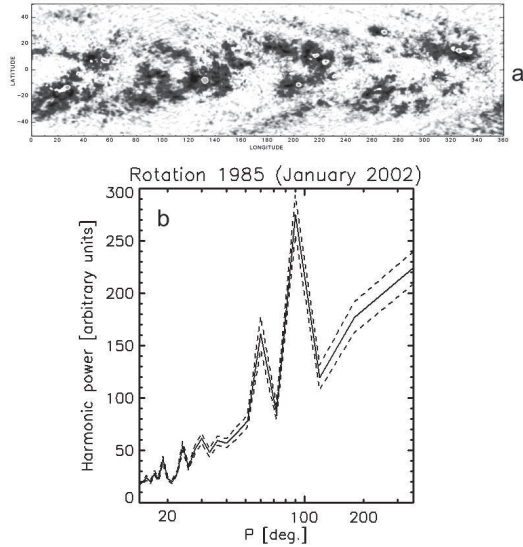


Figure 1: a) Example of used synoptic map of the Fe I line intensity; b) the corresponding average power spectrum of longitudinal variations of activity over the period of a harmonic $P = 360^\circ/m$.

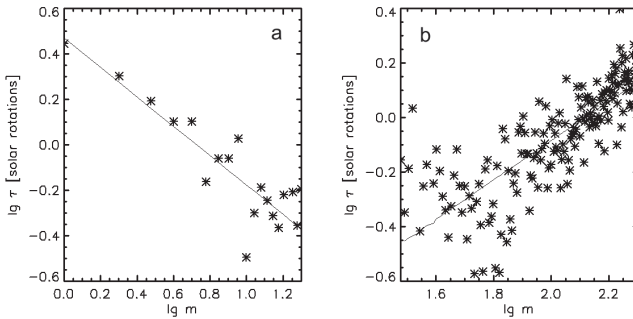


Figure 2: The variability time scale (τ) of the Fourier harmonic of the longitudinal variations in Fe I intensity, when the squared amplitude of the harmonic are used for r_t calculation: a) the Kolmogorov's behavior ($\alpha = -0.65 \pm 0.08$) at $1 \leq m \leq 20$; b) non-Kolmogorov's case ($\alpha = +0.71 \pm 0.04$) at $30 \leq m \leq 200$. The thin lines are found with method of least-squares for the approximation $\lg \tau = C + \alpha \lg m$.

Therefore, the time scale of variability of the large scale solar activity complex decreases with its longitudinal dimension in accordance with the Kolmogorov's theory of turbulence.

This correspondence implies that large magnetic formations split onto smaller structures, etc.

If the super-gigantic complexes of activity are formed without the decay of large scale features into compact ones (as it must be in the turbulent regime), but in inverse order, then the index α can be different from the 'turbulent' value -0.67 . It is important in that respect that the $\tau(m)$ has the non-Kolmogorov's index $\alpha = +0.71 \pm 0.04$ at $30 < m < 200$ (Fig. 2b). This indicates that the short-scale structure of the surface magnetic field is controlled by the horizontal transport of the magnetic field in the photosphere, whereas the large-scale magnetic patterns ($m < 20$) depend on the turbulent processes in the convection zone. Such gigantic ($m < 20$) turbulent motions are typical for deep layers of the convection zone (e.g., Brun et al. [2004, 2008]), but not for the photosphere where even super-granules have diameters only $\sim 3 \times 10^4$ km ($m \sim 150$).

The horizontal transport of magnetic fields in the photosphere is too slow for the formation of large-scale complexes. For example, to blur the supergigantic complex of 45° angular semidiameter in longitude (i.e., harmonic $m = 360^\circ / (2 \times 45^\circ) = 4$) into 60° size ($m = 3$), in the case of the usually accepted coefficient of the horizontal diffusion of magnetic field ($\kappa = 600 \text{ km}^2 \text{ s}^{-1}$ or $9.6 \text{ [deg.}^2/P]$; [Wang and Sheeley, 1994]) it will take the time of $[(60^\circ)^2 - (45^\circ)^2] / \kappa = 164.1P$, which is much larger than the life-time of these complexes (i. e., $\tau = 1.58P$ and $1.26P$ in Fig. 2a for $m = 3$ and 4 respectively).

Therefore, the long-scale pattern of the photospheric/chromospheric activity includes the information on the convective motions in deep layers of the solar convection zone, which is available also for millimeter radio telescopes.

3 Gigantic Convection Cells and Preferred Scales

It is believed that complexes of activity are connected with giant convective cells (e.g., Savinkin et al. [2009]). The computational modeling [Brun et al., 2004; Miesch et al., 2008] predicts the maximum of kinetic energy spectrum for the solar convection at the spherical harmonic index of $10 < \ell < 20$ at the depth up to 56,000 km. As the most unstable mode is realized at $m = \ell$ [Yoshimura, 1971], the expected longitudinal scale of convective pattern is $10 < m < 20$.

To detect the manifestation of such convective pattern, we consider the statistics of local peaks in average power spectra of longitudinal variations of the Fe I (5250.2 \AA) intensity. Such latitude-averaged spectrum is constructed for every of 169 maps (1995-2007) like in Figure 3. We processed every average spectrum to select m -harmonics with power $W(m-1) < W(m) > W(m+1)$ and the ratio of $2W(m)/(W(m-1) + W(m+1)) > K$. The threshold $K = 1.2$ is selected as a compromise between the high noise contribution in the histogram with $K = 1.1$ and poor statistics of spectral peaks with $K = 1.3$. The results are summarized in Figure 3a. This histogram has the broad maximum just at $7 \leq m < 25$ corresponding to the predicted scale ($10 < m < 20$) of the turbulent convection cells.

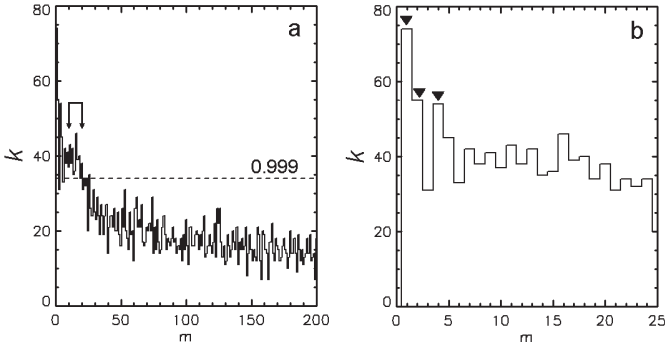


Figure 3: The histograms of local maxima of the power spectra of longitudinal variations of the Fe I line intensity: a) the broad maximum in the histogram coincides with predicted scale of gigantic convection cells (arrowed according to Brun et al.[2004] and Miesch et al. [2008]); b) the details of the histogram maximum in (a) with the narrow peaks of the preferred longitudinal periods (arrowed). The vertical parameter k is the number of spectral maxima in one bin of the histogram. The dashed line in (a) corresponds to the indicated significance levels which are calculated with the Laplace approximation for the binomial distribution of the observed numbers of spectral maxima in the indicated regions of m .

To calculate the significance level of the histogram maximum in Figure 3a, we used the known Laplace approximation for the binomial distribution:

$$P_{k,n} = \frac{1}{\sqrt{2\pi npq}} \exp\left[-\frac{(k - np)^2}{2npq}\right], \tag{1}$$

where $P_{k,n}$ is the probability of k spectral maxima in one histogram bin, n is the total number of spectral maxima in the histogram from $m = 1$ to m_{max} , $p = 1/m_{max}$, and $q = 1 - p$. Then the probability w of $k \leq k_o$ maxima in a bin is

$$w = \sum_{k=0}^{k_o} P_{k,n}. \tag{2}$$

We used $w = 0.999$ level to find the corresponding k of the dashed line in Figure 3a.

Figure 3b shows the details of the histogram maximum in Figure 3a with the peaks corresponding to the preferred longitudinal periods of supergiant complexes of activity at 90° , 180° and 360° . The probability of such accidental deviation from the broad histogram maximum is estimated with $m_{max} = 25$ in Equations 1 and 2 as $1 - w \leq 0.01$. Hence, our analysis confirms the previous reports on these periods in the surface solar activity [Stanek, 1972; Berdyugina, 2006].

These preferred scales could be in connection with standing waves in the rings (tubes) of toroidal magnetic field which are the standard element of the magnetic transport theory (e.g., Caligari [1995, 1998]). If such ring oscillates transversally, it could be an additional

instability factor for the triggering of the tube emersion. Since the number of the standing waves in a ring tube can be only an integer one (n_*), the even numbers of anti-nodes could be associated with the preferred longitudinal scales at $m = 2n_*$ (or $m = 2, 4$ with the periods of 180° and 90°).

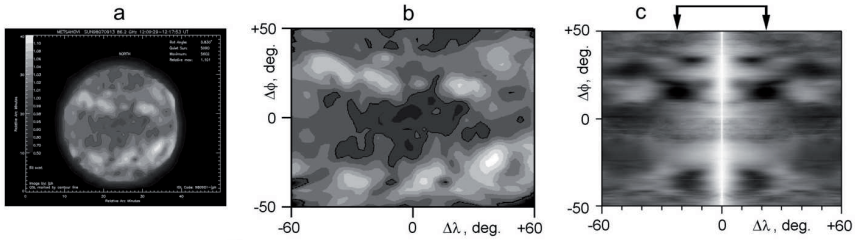


Figure 4: Example of the mm-data processing: a) the initial radio image of the Sun (July 9, 1998, 12:09-18 UT; 86.2 GHz; Metsähovi Observatory); b) the cylindrical equal-area projection of the image; c) the typical autocorrelation pattern for the map in (b) with dark spots of anti-correlation at the longitude shifts of $\Delta\lambda < \pm 45^\circ/2$ (arrowed)

4 What Can be Seen at Millimeter Wavelengths?

The solar chromosphere above active regions have an increased millimeter radio emission (Figure 4a). To demonstrate the manifestations of gigantic cells and preferred scales in mm-data, we apply the autocorrelation method to 188 solar images recorded in the Metsähovi Observatory at 37 GHz and 87 GHz in 1994-1998 (<http://kurp.lut.fi/en/sun/>). Figure 4c shows the typical autocorrelation pattern for the cylindrical map from the Metsähovi solar data. The period of longitudinal variations in mm-emission can be found as the distance between the points with minimal autocorrelation (i.e., anti-correlation) in the scale of longitudinal shift $\Delta\lambda$. One can see the autocorrelation minima (dark spots) at the shifts corresponding to the active region dimension of 30° to 45° .

To study the distribution of active regions with their width and period in longitude, we construct the histogram of $2\Delta\lambda$ for the pixels of autocorrelation minima. Every such pixel is selected with two criteria: $r(\Delta\lambda - d) < r(\Delta\lambda) < r(\Delta\lambda + d)$ and $r(\Delta\lambda) < r_{lim}$, where $r(\Delta\lambda)$ is the coefficient of autocorrelation, $d = 3^\circ$ is the map resolution, and r_{lim} is a formal threshold for the selection. The total histograms of such $2\Delta\lambda$ estimates depict the clear preferred scales at 40° and 90° in Figure 5. The dominating 90° -peak confirms the excess of spectral peaks at $m = 4$ in Figure 3b. The example of such periodicity is shown in Figure 1.

The clear peak in Figure 5 at 40° could be a manifestation of gigantic convection cells. The numerical calculation of time-averaged azimuthal wavenumber (m) spectra of the kinetic energy of turbulent convection at the depth of 35,000 km shows the sharp maximum at $m = 8$, i.e., 45° in longitude [Brun and Toomre, 2002].

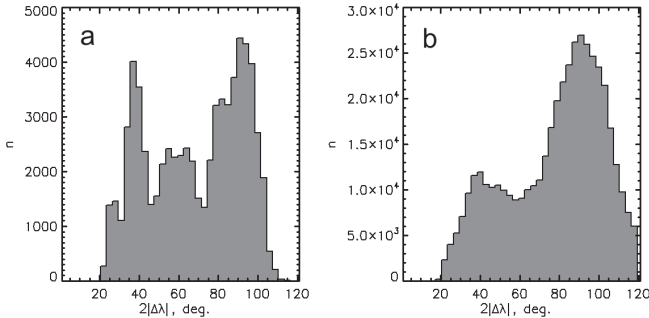


Figure 5: Total histograms of the autocorrelation estimates of longitudinal size of activity complexes: (a) $r_{lim} = -0.5$; (b) $r_{lim} = -0.4$. The vertical parameter n is the number of estimates (i.e., pixels with $r < r_{lim}$ in the dark spots like in Figure 4c) in one bin of the histogram.

5 Conclusions

There are the manifestations of sub-surface motions in the surface activity of the Sun.

1. The Kolmogorov’s turbulence controls the large-scale ($1 < m < 20$) solar surface activity leading to the specific decay of global magnetic formations. This is a signature of the deep convection because there is no such large-scale turbulent eddies in the solar photosphere.
2. The preferred scales of longitudinal variations in solar activity are found at $90^\circ, 180^\circ$ and 360° ($m = 1, 2, 4$ which may be related to global magnetic tube oscillations) and $\sim 15^\circ$ to 51° ($7 \leq m < 25$) corresponding to gigantic convection cells.
3. The solar images, recorded at millimeter wavelenghtes in Metsähovi Observatory, confirm the excess of activity complexes with the longitudinal period of 90° ($m = 4$). Moreover, there is the excess of 40° -complexes in the Metsähovi data of 1994-1998. Such 40° -complexes are interesting for the study of gigantic convection cells.

Hence, the millimeter radio astronomy has certain prospects for remote sensing of the solar convection zone.

Acknowledgements. The authors are thankful to the Academic Exchange program of the Austrian Academy of Sciences for support of their collaboration visits. Both OVAs thank the National Academy of Sciences of Ukraine and Dr. V. P. Churilov for support of this investigation (project "Chadra"; No. 0107U001024). MLK also thanks the Austrian Fonds zur Förderung der Wissenschaftlichen Forschung (project No. P21197-N16).

References

- Berdyugina, S. V., D. Moss, and D. Sokoloff, Active longitudes, nonaxisymmetric dynamos and phase mixing, *Astron. Astrophys.*, **445**, 703–714, 2006.
- Brajsa, R., B. Vrsnak, V. Ruzdjak, S. Jurac, S. Pohjolainen, S. Urpo, and H. Terasranta, Giant Cells on the Sun Revealed by Low Temperature Microwave Regions?, *Hvar Obs. Bull.*, **16**, 1, 1–12, 1992.
- Brun, A. S., and J. Toomre, Turbulent convection under the influence of rotation: sustaining a strong differential rotation, *Astrophys. J.*, **570**, 865–885, 2002.
- Brun, A. S., M. S. Miesch, and J. Toomre, Global-scale turbulent convection and magnetic dynamo action in the solar envelope, *Astrophys. J.*, **614**, 1073–1098, 2004.
- Caligari, P., F. Moreno-Insertis, and M. Schüssler, Emerging flux tubes in the solar convection zone. I. Asymmetry, tilt, and emergence latitude, *Astrophys. J.*, **441**, 886–902, 1995.
- Caligari, P., M. Schüssler, and F. Moreno-Insertis, Emerging flux tubes in the solar convection zone. II. The influence of initial conditions, *Astrophys. J.*, **502**, 481–492, 1998.
- Lang, K. R., *Astrophysical formulae*, Springer-Verlag, Berlin, 1974.
- Laurène, J., and A. S. Brun, Three-Dimensional Nonlinear Evolution of a Magnetic Flux Tube in a Spherical Shell: Influence of Turbulent Convection and Associated Mean Flows, *Astrophys. J.*, **701**, 1300–1322, 2009.
- Miesch, M. S., A. S. Brun, M. L. DeRosa, and J. Toomre, Structure and evolution of giant cells in global models of solar convection, *Astrophys. J.*, **673**, 557–575, 2008.
- Savinkin, M. Yu., V. I. Sidorov, and S. A. Yazev, Unique complex of activity between 2006 and 2007, *Geomagn. Aeron.*, **49**, 1072–1075, 2009.
- Stanek, W., Periodicities in the Longitude Distribution of Sunspots, *Solar Phys.*, **27**, 1, 89–106, 1972.
- Tobias, S. M., The solar dynamo, *Phil. Trans. R. Soc. Lond.*, **360**, 1801, 2741–2756, 2002.
- Vrsnak, B., S. Pohjolainen, S. Urpo, H. Terasranta, R. Brajsa, V. Ruzdjak, Z. Mouradian, and S. Jurac, Large-scale patterns on the sun observed in the millimetric wavelength range, *Solar Phys.*, **137**, 67–86, 1992.
- Wang, Y.-M., and N. R. Sheeley, The rotation of photospheric magnetic fields: a random walk transport model, *Astrophys. J.*, **430**, 399–412, 1994.
- Williams, P. E., and M. Cuntz, A method for the treatment of supergranulation advection by giant cells, *Astron. Astrophys.*, **505**, 1265–1268, 2009.
- Yoshimura, H., Complexes of Activity of the Solar Cycle and Very Large Scale Convection, *Solar Phys.*, **18**, 417–433, 1971.